Rare Metal Materials and Engineering
Volume 48, Issue 1, January 2019
Available online at www.rmme.ac.cn

Science Press

Cite this article as: Rare Metal Materials and Engineering, 2019, 48(1): 0104-0110

ARTICLE

Effect of 0.12wt% Hydrogen Addition on Microstructural Evolution of Ti-0.3Mo-0.8Ni Alloy Argon-arc Welded Joints

Zhang Zhaohui[1], Liu Quanming[1], Liu Shifeng[1], Yang Haiying[2]

[1] Xi'an University of Architecture and Technology, Xi'an 710055, China; [2] Northwest Institute for Nonferrous Metal Research, Xi'an 710016, China

Abstract: The effects of hydrogen addition (0.12 wt% H) on microstructural evolution in Ti-0.3Mo-0.8Ni alloy argon-arc welded joints have been investigated using optical microscope (OM), X-ray diffraction (XRD) and transmission electron microscopy (TEM) to reveal the influence of hydrogen on the characteristics of defect-free titanium alloy welded joints. The results show that hydride precipitation changes the initial microstructure of the welded joints. The increase of hydrogen content is favorable for the β phase precipitation. Face centered cubic δ hydride is evenly distributed in the hydrogenated 0.12 wt% H welded joints. The lamellar δ hydride could only precipitate from the lamellae α, and not from the transformed β phase. Formation of δ hydride is associated with the result of α_H phase separation reaction: $\alpha_H \rightarrow \alpha$ (H lean region) + δ (H rich region), and H rich regions finally transform to the δ phase. The dislocation distribution is heterogeneous and there is a relatively high density of dislocations in the vicinity of the precipitated δ hydride, which are caused by the lattice distortion due to the stress field generated by the hydride precipitation.

Key words: titanium alloy; welded joints; hydrogenation; microstructure; δ hydride

Titanium alloys are widely used in the aerospace, industry, marine and commercial applications due to their high specific strength to weight ratio combined with excellent corrosion and fatigue crack growth resistances[1-3]. Hydrogen is a very active chemical element and has a strong affinity with titanium alloys, and the hydrides can be precipitated with increasing hydrogen content[4]. Previous researches have shown that three kinds of precipitated hydrides, with different structures and different hydrogen concentrations in titanium alloy: (1) face centered tetragonal (fct) γ hydride TiH with $c/a>1$ at low hydrogen concentration, (2) face centered cubic (fcc) δ hydride TiHx ($1.50<x<1.99$) at intermediate hydrogen concentration, and (3) face centered tetragonal (fct) ε hydride TiH_2 with $c/a<1$ at high hydrogen concentration[5]. Titanium equipments are widely used when the components are exposed to hydrogen environments. Hydrogen addition has considerable effect on the microstructures and mechanical properties of titanium alloys. With the popularity of titanium equipment[6], welding technology has been the necessary means of equipment support and manufacturing. Since the beginning of the titanium industry, much attention has been paid to microstructural evolution, phase transformation and mechanical properties of the hydrogenated single titanium alloys[7-9] and un-hydrogenated titanium alloy welded joints[10-13]. Most of the academic publications have focused on the hydride formation of the hydrogenated single titanium alloys[14-16].

However, little work has been reported on the effect of hydrogen addition on microstructural evolution of the titanium alloy welded joints[17]. Studies on microstructural evolution in titanium alloy welded joints are even more sporadic, especially for low hydrogenation content commonly used in practice. In

Received date: January 09, 2018
Foundation item: National Natural Science Foundation of China (51671152)
Corresponding author: Liu Quanming, Candidate for Ph. D., School of Metallurgical Engineering, Xi'an University of Architecture and Technology, Xi'an 710055, P. R. China, E-mail: liuquanming1988@126.com

this research, the hydrogenated Ti-0.3Mo-0.8Ni alloy argon-arc welded joints with 0.12 wt% H demonstrated the effect of hydrogen addition on microstructural evolution of the titanium alloy welded joints. Meanwhile, this study will also be helpful to guide the safety design, materials selection and corrosion prevention of titanium equipments.

1 Experiment

The test material was a 10 mm-thick, mill-annealed Ti-0.3Mo-0.8Ni alloy sheet with chemical composition of Mo 0.32, Ni 0.75, Fe 0.08, O 0.014, C 0.01, N 0.03, H 0.004 and Ti balance (mass fraction, %), which has been widely applied in the manufacturing field of chemical containers and marine equipments. The beta transition temperature for the material is 880 °C measured by the metallographic method. The surfaces of thick sheets to be welded were brushed and then cleaned with ethanol to remove any previous oxides and/or surface contaminations that may adversely affect the integrity of the weldments. Manual GTAW welding process was employed for welding using filler wires with 2.5 mm in diameter, and the welding was carried out in a clean room with continuous purging of ultrapure (99.99% purity) argon gas, providing the shielding, trailing and backing actions. The welded joint using DCEN polarity with a Thoriated Tungsten welding torch was obtained in a multipass weld with the same welding process parameters as follows: welding current of 130 A, welding voltage of 20 V, traveling speed of 10 $cm \cdot min^{-1}$ and argon gas shielding at 50 $L \cdot min^{-1}$. After welding, the weld joint position was examined to ensure no obvious welding defects caused by ultrasonic inspection. Rectangular bars with 70 mm×10 mm×10 mm (length×width×thickness) in dimension were taken and machined from argon-arc welded Ti-0.3Mo-0.8Ni alloy thick sheets, and the sampling schematic is shown in Fig.1a.

The certain hydrogen content was obtained rapidly by thermo-hydrogen processing, which was used to simulate the accumulation of hydrogen content in the long-term using titanium containers exposed to hydrogen environments, and the influence of hydrogen on titanium alloy welded joints further revealed the premature vehicle failure and associated accidents of titanium containers. The 0.12wt% hydrogen addition was investigated in this paper; meanwhile, the as-received specimens were introduced as the contrast specimens. According to the Ti-H phase diagram[18], considering the valuable phase transformation during furnace cooling of the hydrogenated welded joints, the 0.12 wt% H was a typical hydrogen content. On the other hand, based on the case analysis in Ref. [19], titanium equipments could lead to hydrogen embrittlement between 0.008 wt%~1.5 wt% hydrogen additions, but especially for titanium containers, low hydrogen concentration environments are most typically encountered in practice, and 0.12 wt% H also had practical application value.

Specimens were hydrogenated using the following procedures: (1) The surface oxides were removed via grinding and ultrasonic cleaning with acetone. (2) Specimens were hydrogenated at 750 °C by being held in a purified hydrogen environment for 2 h, and then were moved to the furnace cooling area to room temperature. Specimens with 0.12 wt% H were obtained by controlling the hydrogen pressure, and hydrogen concentrations were determined by weighing of the specimen before and after hydrogenation to the nearest 0.01 mg[20]. After hydrogenation, the hydrogenated and un-hydrogenated rectangular bars with dimensions of 6 mm×6 mm×10 mm (length×thickness×width) for OM observations and XRD analysis were changed from the bar with dimensions of 70 mm×10 mm×10 mm (length×width×thickness), and the sampling schematic is shown in Fig.1b. Specimens were ground, mechanically polished and finally etched in a solution of $V(HF):V(HNO_3):V(H_2O)$ =1:3:7. Observations were made on an Axio Vert A1 optical microscope. The center of rectangular bars with dimensions of 6 mm×6 mm×10 mm (length×thickness×width) were selected for TEM observations. TEM foils were mechanically thinned to approximately 50 μm and then sliced into a 3 mm-diameter circle. Then, an additional thickness reduction was carried out using a Struers Tenupol-5 twin-jet electrolytic polisher in a solution of 6% perchloric acid + 34% butyl alcohol +60%

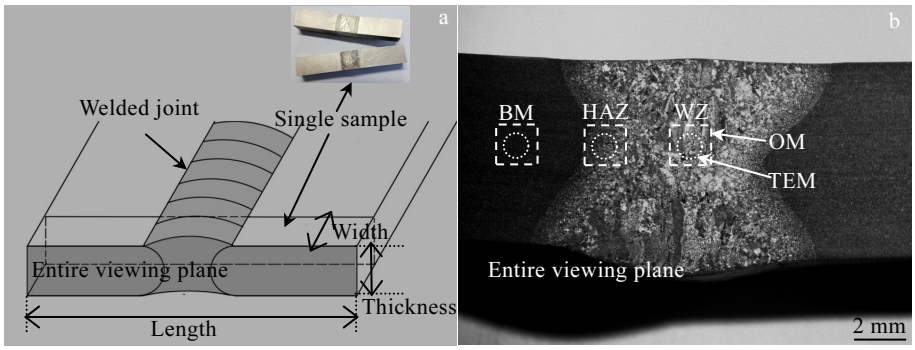

Fig.1 Sampling schematic of the welded joints: (a) a single specimen and (b) OM/TEM viewing zone in low magnification

methanol (vol%) between −10 and −20 °C. TEM analysis was performed using a Tecnai F20 transmission electron microscope operated at 200 kV. The precipitated hydride phases into the center of the fusion zone were examined via the Bruker D8 Advance ECO A25 X-ray diffractometer using a Cu Kα radiation of 0.154 nm wavelength at an accelerating voltage of 40 kV and a current of 40 mA, with the 2θ scan ranging from 30° to 80° at the speed of 0.15 s/step, and a step size of 2θ=0.02°.

2 Results and Discussion

2.1 Optical microstructure observation

OM observations for the welded joints with the as-received and 0.12 wt% H are shown in Fig.2. The initial microstructure of the welded joints was divided into three distinct areas, including the fusion zone (FZ), the heat-affected zone (HAZ) and the base material (BM). The as-received BM had an initial microstructure with the rolled (α+β) biphasic structure, a few of beta phase (dark dots, Fig.2a) were uniformly distributed on the alpha phase matrix (white regions, Fig.2a) in dots, and there were no complete grain boundaries (black lumps, Fig.2a) of prior alpha phases due to incomplete recrystallization of alpha phases caused by the annealing temperature being lower than transformation temperature. For the as-received HAZ, high temperature produced by argon-arc welding process led to further solid solution treatment and the initial microstructure was composed of a mixed alpha phases of equiaxed and lamellar, and a few beta phases uniformly distributed on the alpha phase (Fig.2b). For the as-received FZ, high temperature produced by argon-arc welding process was obviously higher than beta phase transformation temperature, because the initial microstructure exhibited alpha lamellae with a transformed beta phase present at colony boundaries. The grain boundary of the prior beta grain was completely preserved, alpha lamellae was arranged in a certain orientation, and when several of these “alpha lamellas” were aligned in parallel, they formed so called “colonies”, which appeared in prior beta grain images (Fig.2c). The process of hydrogen treatment at a high temperature for the welded joints was considered over another solid solution treatment. With a further increase of hydrogen content, hydride precipitation could also change the initial microstructure of the welded joints. As shown in Fig.2d, 2e, short acicular phases (black acicular, Fig.2d, 2e) associated with hydride precipitation could have precipitated from the microstructure of the hydrogenated welded joints with 0.12 wt% H. The precipitated short acicular phases were arranged in a randomly disordered fashion in the hydrogenated BM (Fig. 2d), but most of short acicular phases emerged with a regular arrangement along the orientation of alpha lamellae in the hydrogenated HAZ and FZ (Fig. 2e and 2f), nucleated and grew inside prior beta grain (Fig. 2d, 2e and 2f). Differences between nucleation and growth of short acicular phases in the hydrogenated BM and HAZ/FZ were closely related to recrystallization process during welding. With hydrogen treatment at a high temperature for the welded joints, in addition to the short acicular phases, the hydrogenated BM had an initial microstructure of equiaxed alpha phase produced by further recrystallization of alpha phase matrix and a few of the beta phase (Fig.2d), but the microstructure of the hydrogenated HAZ and FZ was not significantly changed before or after hydrogen treatment (Fig.2e and 2f). However, based on additional dark dots in the hydrogenated welded joints with 0.12 wt% H (Fig.2f) compared to the as-received welded joints (Fig.2c), the increase in hydrogen content was more favorable for the beta phase precipitation. Hydrogen as a beta stable element could stabilize the beta phase and decrease beta transition temperature[21] during the occurrence of the $\alpha\rightarrow\beta$ phase transformation. The increase in the number of plastic beta phase could cause a reduction in yield strength of the welded joints. The short acicular phases had been associated with the hydride precipitation by the possible $\alpha_H\rightarrow\alpha+\delta$ and $\beta_H\rightarrow\alpha+\delta$ phase transformations, which were subsequently supported by the XRD and TEM analysis.

2.2 XRD analysis

The X-ray diffraction patterns of Ti-0.3Mo-0.8Ni alloy argon-arc welded joints for the fusion zone that contains the as-received and 0.12 wt% H are shown in Fig.3. As shown in Fig.3a, the original material only shows a simple XRD with a hexagonal close-packed alpha phase and body-centered cubic beta phase. The Ti-H phase diagram[18] indicated the hydrogen saturation in the alpha phase (4.7 at% H) was much lower than that in the beta phase (42.5 at% H), and thus the hydride first precipitated in the alpha phase. As presented by Fig.3b, for the hydrogenated fusion zone with 0.12 wt% H (5.41 at% H) exceeding hydrogen saturation in the alpha phase, the peak of the hydride obviously appeared at 2θ=40.585° and 2θ=58.804°. The hydride was indexed as a face-centered cubic (fcc) δ hydride with the calculated lattice parameter of a=0.444 nm. Its composition ranged from $TiH_{1.5}$ to $TiH_{1.99}$. The δ hydride has a CaF_2 type structure with titanium atoms on an fcc lattice and hydrogen atoms randomly occupying tetrahedral interstitial sites[22]. As shown in Fig.3a and 3b, with the hydrogen content further increasing, the XRD peaks of alpha phase had not significant change in location because the low hydrogen solubility in alpha phase caused by each cell had only four tetrahedral interstitial sites and two octahedral interstitial sites in HCP alpha phase[23]. The δ hydride precipitation obviously showed that some XRD peaks of alpha phase were broadened after hydrogenation due to building up a high microscopic internal stress field (Fig.3b, red box).

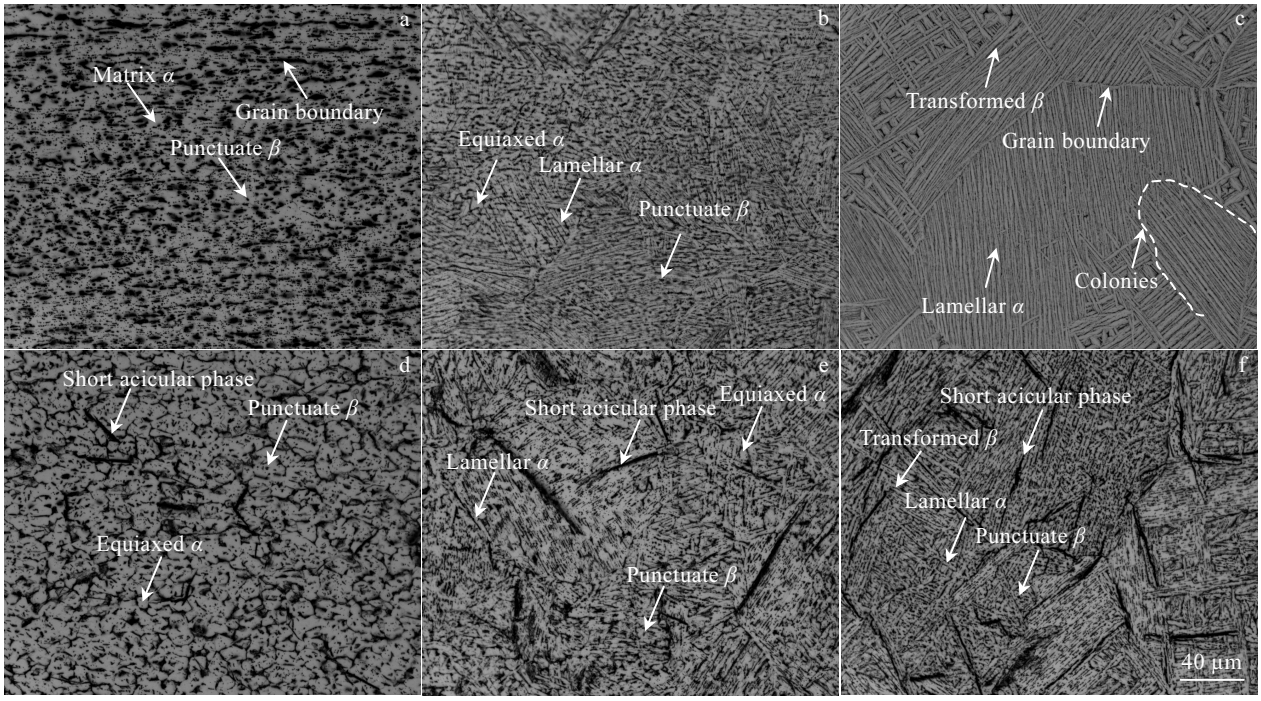

Fig.2 OM images of different zones for the welded joints: (a), (b), (c) is the as-received BM, HAZ, FZ, respectively and (d), (e), (f) is BM, HAZ, FZ with 0.12 wt% H, respectively

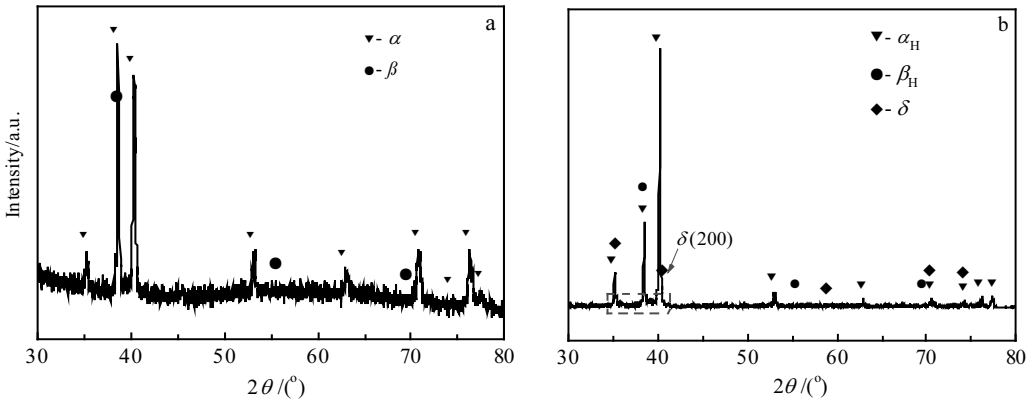

Fig.3 XRD patterns for the fusion zone of the welded joints: (a) the as-received and (b) with 0.12 wt%

2.3 TEM investigation

Based on the hydride uniformly distributed on three distinct areas of the welded joints, the fusion zone was selected as a typical observation area of TEM. More detailed microstructural information the hydrogenated fusion zone with 0.12 wt% H is given in Fig.4. As shown in Fig.4a and 4c, TEM observation indicated obvious hydride precipitation from alpha lamellae during hydrogen treatment at high temperatures, which were then cooled to room temperature. The lamellar δ hydride grew approximately parallel into alpha matrix (Fig.4a and 4c). As shown in Fig.4b and 4d, the corresponding selected area electron diffraction (SAED) pattern suggested an fcc structure with a $[01\bar{1}]$ and [255] zone axis for the δ hydride. The lattice parameter of δ hydride calculated in terms of the SAED pattern was 0.444 nm, which agreed with a CaF_2 type structure. As shown in Fig.4a and 4c, lamellar δ hydride have precipitated from alpha lamellae, the δ hydride formation might be associated with α_H phase separation reaction: $\alpha_H \rightarrow \alpha$ (H lean region)+ δ (H rich region), and H rich regions transformed to the δ phase. Lamellar hydride grew via the supply of hydrogen atoms from alpha lamellae interval. However, as shown in Fig.4a, for a transformed beta phase, there are no hydride precipitation from the transformed beta phase until cooled to room temperature because

of the high hydrogen solubility in the beta phase compared to the hydrogen content of the hydrogenated fusion zone with 0.12 wt% H.

2.4 Substructural characteristics

TEM images of the typical region in the welded joints containing the as-received and 0.12 wt% H are shown in Fig.5, which illustrated the influence of hydrogen addition on the internal substructural characteristics around

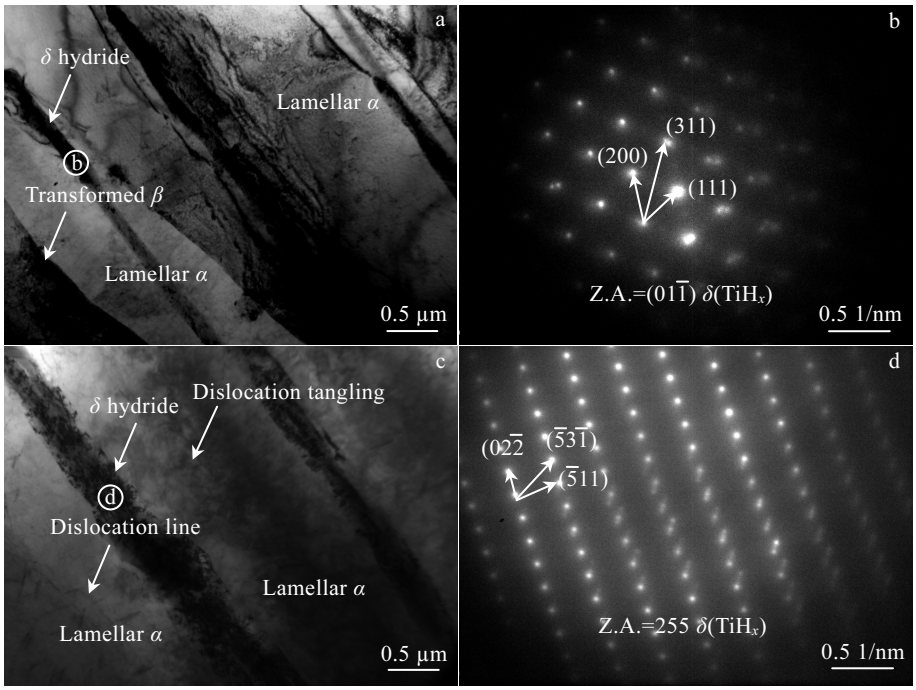

Fig.4 TEM images for the fusion zone of the welded joints with 0.12 wt% H: (a) BF micrograph of lamellar δ hydride, (b) SAED pattern of lamellar δ hydride, (c) BF micrograph of another δ hydride, and (d) SAED pattern of another δ hydride

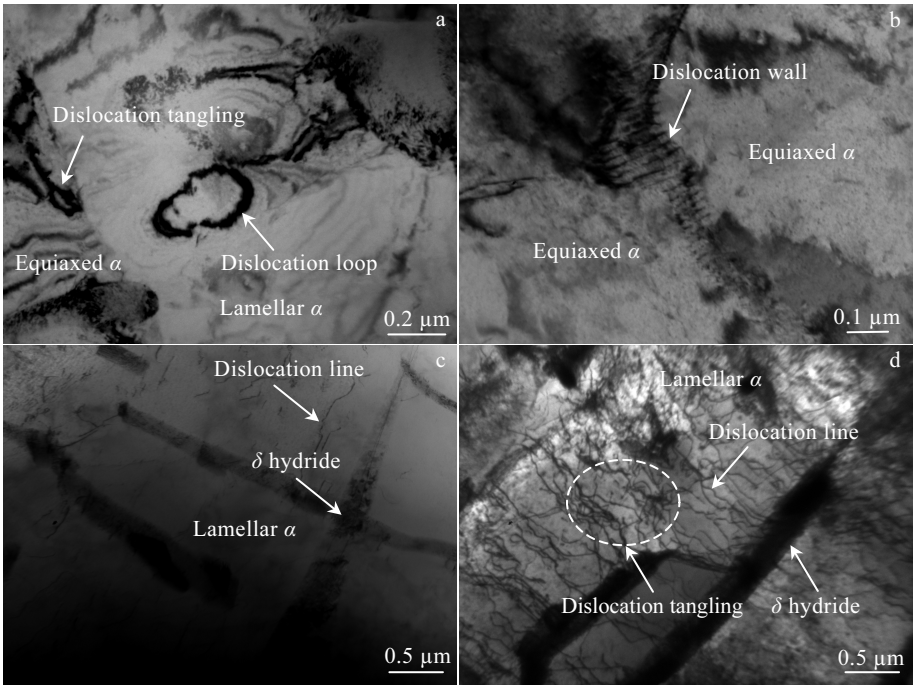

Fig.5 TEM images of the welded joints: (a) BF micrograph of the as-received HAZ, (b) BF micrograph of the as-received BM, (c, d) BF micrograph of the FZ and BM with 0.12 wt% H

the δ hydride. As shown in Fig.5a, the dislocation tangling with the high density, dislocation loops and dislocation walls were found in the as-received welded joints. However, considering the strong interaction between hydrogen and dislocation, a high temperature could promote the dislocation movement, thus reducing dislocation density of titanium alloy. As shown in Fig.5b, the dislocation density of the welded joints with 0.12 wt% H was decreased significantly, and only a small number of dislocation lines were sporadically scattered around the precipitated δ hydride (Fig.5c). On the other hand, the δ hydride precipitated from alpha lamellae, and a large number of dislocations were found in the vicinity of the region where the δ hydride was concentrated (Fig.5d). This was caused by the lattice distortion due to stress field generated by hydride precipitation. As seen from Fig.5c and 5d, the dislocation distribution was heterogeneous and there was a relatively high density of dislocations in the vicinity of the precipitated δ hydride as well as dislocation propagation characteristics in some parts of the interface between the δ hydride and alpha matrix. Therefore, the dislocation configuration change was caused by the presence of δ hydride.

Considering the dislocation configuration change caused by the presence of δ hydride, but compared with strengthening effect of the precipitated δ hydride and more dislocations around it (Dislocation movement was hindered by δ hydride) for the welded joints, the main reason for the phenomenon that the yield strength of the hydrogenated welded joints with 0.12 wt% H decreased slightly lay in the leading role in the softening of the beta phase.

3 Conclusions

1) The hydride precipitation changes the initial microstructure of Ti-0.3Mo-0.8Ni alloy argon-arc welded joints, and the increase in hydrogen content is more favorable for the beta phase precipitation.

2) Face-centered cubic δ hydride phase is found in the hydrogenated 0.12 wt% H fusion zone. The lamellar δ hydride could only precipitate from the alpha lamellae, but not from the transformed beta phase due to the high hydrogen solubility found in the beta phase.

3) Formation of δ hydride is associated with the result of α_H phase separation reaction: $\alpha_H \rightarrow \alpha$ (H lean region)+δ (H rich region), and H rich regions finally transform to the δ phase.

4) The hydrogenation process can promote the dislocation movement and thus reduce the dislocation density of the fusion zone. The dislocation distribution was heterogeneous and there is a relatively high density of dislocations in the vicinity of the precipitated δ hydride, which are caused by the lattice distortion due to the stress field generated by the hydride precipitation.

Acknowledgement: The authors would like to gratefully acknowledge in support of Northwest Institute for Non-ferrous Metal Research. The authors would also like to thank the researcher in China Aeronautical Manufacturing Technology Research Institute, Y. Q. Wang for hydrogenation, and the researchers at Xi'an University of Architecture and Technology, M. Yang and X. S. Ding for fruitful discussions.

References

1 Crupi V, Epasto G, Guglielmino E *et al. International Journal of Fatigue*[J], 2016, 95: 64
2 Zhang Z H, Liu Q M, Yang H Y *et al. Journal of Materials Engineering and Performance*[J], 2017, 26(7): 3368
3 Guo Ping, Zhao Yongqing, Zeng Weidong. *Rare Metal Materials & Engineering*[J], 2015, 44(2): 277 (in Chinese)
4 Eliezer D, Tal-Gutelmacher E, Cross C E *et al. Materials Science and Engineering A*[J], 2006, 433(1-2): 298
5 Chen C Q, Li S X, Lu K. *Acta Materialia*[J], 2003, 51(4): 931
6 Liu W Y, Lin Y H, Chen Y H *et al*. *Rare Metal Materials and Engineering*[J], 2017, 46(3): 634 (in Chinese)
7 Chen R R, Ma T F, Guo J J *et al. Materials & Design*[J], 2016, 108: 259
8 Zong Y Y, Liang Y C, Yin Z W *et al. International Journal of Hydrogen Energy*[J], 2012, 37(18): 13631
9 Leonardo Contri Campanelli, Alberto Moreira Jorge Jr, Claudemiro Bolfarini. *Scripta Materialia*[J], 2017, 132: 39
10 Wang S Q, Li W Y, Jing K *et al. Materials Science and Engineering A*[J], 2017, 697: 224
11 Ma T J, Li X, Zhong B *et al. Science & Technology of Welding & Joining*[J], 2014, 19(8): 689
12 Wu Bing, Li Jinwen, Tang Zhenyun. *Rare Metal Materials & Engineering*[J], 2014, 43(4): 786 (in Chinese)
13 Huang Z T, Suo H B, Yang G *et al*. *Rare Metal Materials and Engineering*[J], 2017, 46(3): 760 (in Chinese)
14 Li X, Jiang J, Wang S *et al. International Journal of Hydrogen Energy*[J], 2017, 42(9): 6338
15 Li Z, Ou P, Sun N *et al. Materials Letters*[J], 2013, 105(16): 16
16 Shen C C, Wang C M. *Journal of Alloys & Compounds*[J], 2014, 601: 274
17 Zhou L, Liu H J. *Materials Characterization*[J], 2011, 62(11): 1036
18 Manchester F D, San-Martin A. *Phase Diagrams of Binary Hydrogen Alloys*[M]. Materials Park: ASM International, 2000: 238
19 Yu C Y. *Process Equipment & Piping*[J], 2010, 47(2): 53 (in Chinese)
20 Senkov O N, Froes F H. *International Journal of Hydrogen Energy*[J], 1999, 24(6): 565
21 Qazi J I, Rahim J, Fores F H *et al. Metallurgical & Materials*

Transactions A[J], 2001, 32(10): 2453
22 Numakura H, Koiwa M. *Acta Metallurgica*[J], 1984, 32(10): 1799
23 Elias R J, Corso H L, Gervasoni J L. *International Journal of Hydrogen Energy*[J], 2002, 27(1): 91

置氢 0.12wt% H 对 Ti-0.3Mo-0.8Ni 氩弧焊接接头组织演变的影响

张朝晖[1]，刘全明[1]，刘世锋[1]，杨海瑛[2]
(1. 西安建筑科技大学，陕西 西安 710055)
(2. 西北有色金属研究院，陕西 西安 710016)

摘 要：基于光学显微镜、X 射线衍射仪和透射电子显微镜分析，研究了置氢 0.12 wt% H 对 Ti-0.3Mo-0.8Ni 氩弧焊接接头微观组织演变影响，揭示了氢元素对无损焊接接头组织特性影响规律。结果表明：氢化物析出促使焊接接头初始组织发生变化，置氢量增加有助于焊接接头微观组织中 β 相析出。薄片状的面心立方 δ 氢化物均匀分布在置氢量为 0.12 wt% H 的焊接接头中，且仅能从层片状 α 相中析出，但无法从转变 β 相中析出。δ 氢化物的析出与 α_H 相分解反应：$\alpha_H \rightarrow \alpha$ (贫氢区) + δ (富氢区)相关，富氢区最终转变为 δ 氢化物. 置氢焊接接头组织中的位错分布不均匀，δ 氢化物析出产生的应力场引起的晶格畸变直接导致了析出 δ 氢化物附近有相对密度高的位错分布。

关键词：钛合金；焊接接头；置氢处理；微观组织；δ氢化物

作者简介：张朝晖, 男, 1967 年生, 博士, 教授, 西安建筑科技大学冶金工程学院，陕西 西安 710055，E-mail: zhzhhui67@126.com